

THE INFLUENCE OF MACROSCOPIC AND MICROSCOPIC FIBRE ORIENTATION DISPERSION ON DIFFUSION MR MEASUREMENTS: A MONTE-CARLO SIMULATION STUDY

Tingting Wang¹, Hui Zhang¹, Matt G. Hall¹, and Daniel C. Alexander¹
¹University College London, London, United Kingdom

Target audience: researchers working on diffusion MRI, biophysical modelling and tractography.

Purpose: We compare and contrast the effects of different types of fibre orientation dispersion on microstructural parameter estimates from diffusion MRI. In biological tissue, fibre orientation dispersion can be divided into two classes: 1) Macroscopic fibre dispersion, a population of straight fibres with different orientation, such as in crossing and fanning structures. 2) Microscopic fibre dispersion, individual fibres with varying orientation, such as undulating fibres, which are common in nerve tissue to accommodate stretching during movement [1]. Measuring orientation dispersion is useful both for characterizing the spatial arrangement of neuronal processes but also for estimating other microstructural features, such as axon diameter and density accurately [2]. Recent parametric models of dispersion enable such estimation [3, 4, 5]. However, these works implicitly assume macroscopic dispersion. In the presence of microscopic dispersion, this assumption may bias the microstructural parameter estimates [6] but the exact effects are yet to be studied. Here we construct virtual white matter environments for each type of dispersion and conduct Monte-Carlo diffusion simulations to study differences that arise in the water dispersion, standard Diffusion Tensor Imaging (DTI) [7] indices, and parameter estimates from current biophysical models of fibre dispersion.

Methods: We construct mesh fibres with biologically realistic structure and Watson Orientation Distribution Function (ODF) and then use the Monte-Carlo simulator [8] in the Camino diffusion MRI toolkit [9]. Macroscopic dispersion substrates contain straight cylinders with orientations \mathbf{n}_k , $k=1, \dots, K$ drawn from a Watson distribution. Microscopic dispersion substrates consist of a single undulating cylinder assembled by joining straight segments with orientations $\mathbf{n}_1, \dots, \mathbf{n}_K$. We control the dispersion scale of Micro substrates by varying segment length l , and the dispersion amplitude by increasing the likelihood that consecutive segments have similar orientation. We test three Micro substrates, Micro1, Micro2 and Micro3, with the same Watson orientation distribution but decreasing amplitude. Fig.1 shows substrates for one set of \mathbf{n}_k from a Watson distribution with dispersion parameter $\kappa = 4$. All substrates have axon diameter $a = 6\mu\text{m}$. We synthesize data from the ActiveAx stimulated echo acquisition protocol in Alexander et al. [10] which contains 3 HARDI shells: $b\text{-value} \in \{2306, 3425, 14631\} \text{ s/mm}^2$, gradient strength $\in \{260.4, 300.00, 113.50\} \text{ mT/m}$ and diffusion time $\in \{150.64, 16.33, 150.14\} \text{ ms}$. We use the $b = 3425 \text{ s/mm}^2$ shell alone for DTI. The simulation uses only intra-cellular spins with diffusivity $6 \times 10^4 \text{ mm}^2/\text{s}$. We fit the Delta and Watson dispersion models in Zhang et al. [2] to estimate fibre diameter and dispersion.

Experiments and results: Fig.2 plots parameter estimates from Macro and each Micro with $l = 4\mu\text{m}$ and $\kappa \in \{3, 4, 5, 6\}$. The error bars show variation over 10 different random draws of the \mathbf{n}_k . For Macro we recover the ground truth κ (Fig.2b) correctly, whereas we overestimate κ for microscopic dispersion and the overestimation increases as the dispersion amplitude decreases. This increase in anisotropy is also reflected by the increase in FA (Fig.2a). As Zhang et al. [2] shows previously, the Delta model overestimates a (Fig.2c); the bias is largest for Macro, and smallest for Micro3. Fig.3 plots estimated a and κ for Micro substrates with $\kappa = 4$ and $l \in \{4, 10, 30, 50, 100\} \mu\text{m}$. Overestimation of a (Fig.3a) with the Delta model increases with l and is largest in Micro1. The Watson model more accurately recovers a in all cases, but overestimates κ (Fig.3b) for short l , with largest bias for Micro3. The bias gradually decreases as l increases, and the estimation converges to ground truth value when $l \geq 30 \mu\text{m}$, at about the root-mean squared displacement (RMSD).

Discussion and conclusion: We demonstrate that different types of fibre dispersion affect parameters derived from diffusion MR reconstruction techniques differently. At large scale, i.e. l at or above RMSD, microscopic dispersion produces diffusion behaviour similar to macroscopic dispersion, but at small scale it appears more anisotropic. Fig.4 confirms this trend. The transition in behaviour occurs around $l = \text{RMSD}$, because above this value, spins rarely exchange between segments with different orientations, whereas below they exchange often. The parameter κ expresses the fibre ODF, which is important in tractography. Our results suggest that, using current methods, the ODF can be recovered accurately in macroscopic dispersion, but not with small scale microscopic dispersion. We suggest considering such effects in future modelling works. Here we test only one acquisition protocol, but the choice of diffusion times is important to define the scale and transition point in behaviour. **References:** 1. Fontana *Florence1781*. 2. Zhang et al. *NIMG11*. 3. Kaden et al. *NIMG07*. 4. Sotiropoulos et al. *NIMG12*. 5. Zhang et al. *NIMG12*. 6. Nilsson et al. *NMRBiomed12*. 7. Basser et al. *BiopJ94*. 8. Hall et al. *TMI09*. 9. Cook et al. *ISMRM06*. 10. Alexander et al. *ISMRM12*.

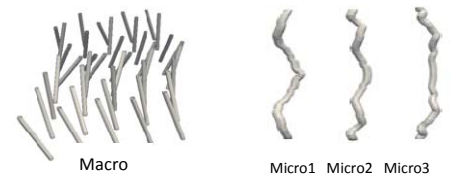


Fig. 1: Macro substrate (left) and Micro substrates (right). Micro1, Micro2 and Micro3 are three Micro substrates with the same ODF but decreasing amplitudes.

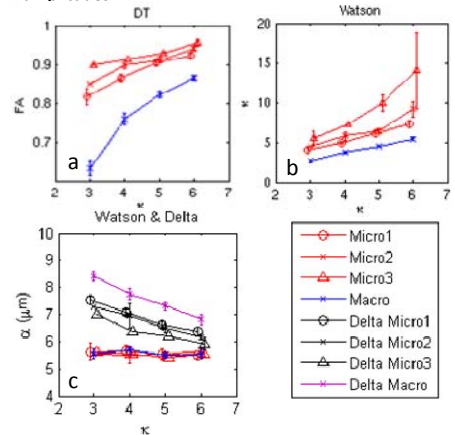


Fig. 2: Estimate of (a) FA and (b) Watson dispersion parameter, for Macro and Micro. (c) plots the estimated diameter from Watson and Delta model (should be about $6\mu\text{m}$).

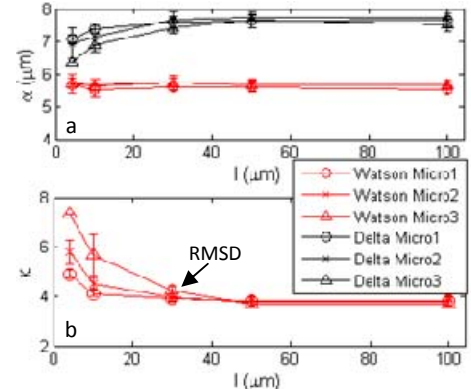


Fig. 3: Recovery of (a) a and (b) κ for Micro substrates with $\kappa = 4$ and a varying segment length l , showing the trends from microscopic to macroscopic dispersion.

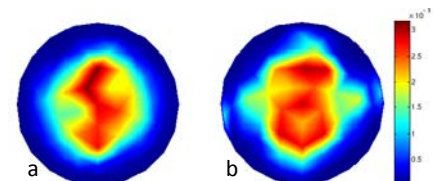


Fig. 4: Spin displacement distribution of (a) small scale Micro $l = 4 \mu\text{m}$ and (b) large scale Micro $l = 100\mu\text{m}$. (a) shows greater concentration than (b).